LETTERS

Intense mixing of lower thermocline water on the crest of the Mid-Atlantic Ridge

Louis C. St Laurent[1] & Andreas M. Thurnherr[2]

Buoyancy exchange between the deep and the upper ocean, which is essential for maintaining global ocean circulation, mainly occurs through turbulent mixing[1,2]. This mixing is thought to result primarily from instability of the oceanic internal wave field[3], but internal waves tend to radiate energy away from the regions in which they are generated rather than dissipate it locally as turbulence[4] and the resulting distribution of turbulent mixing remains unknown. Another, more direct, mixing mechanism involves the generation of turbulence as strong flows pass through narrow passages in topography, but the amount of turbulence generated at such locations remains poorly quantified owing to a lack of direct measurements. Here we present observations from the crest of the Mid-Atlantic Ridge in the subtropical North Atlantic Ocean that suggest that passages in rift valleys and ridge-flank canyons provide the most energetic sites for oceanic turbulence. Our measurements show that diffusivities as large as $0.03\,m^2\,s^{-1}$ characterize the mixing downstream of a sill in a well-stratified boundary layer, with mixing levels remaining of the order of $10^{-4}\,m^2\,s^{-1}$ at the base of the main thermocline. These mixing rates are significantly higher than the diffusivities of the order of $10^{-5}\,m^2\,s^{-1}$ that characterize much of the global thermocline and the abyssal ocean[5]. Our estimates suggest that overflows associated with narrow passages on the Mid-Atlantic Ridge in the North Atlantic Ocean produce as much buoyancy flux as has previously been estimated for the entire Romanche fracture zone[6,7], a large strait in the Mid-Atlantic Ridge that connects the North and South Atlantic basins. This flux is equivalent to the interior mixing that occurs in the entire North Atlantic basin at the depth of the passages, suggesting that turbulence generated in narrow passages on mid-ocean ridges may be important for buoyancy flux at the global scale.

We focused on the upper layer of North Atlantic Deep Water, originating in the Greenland, Iceland and Norwegian seas. While some North Atlantic Deep Water flows south in a deep western boundary current along Labrador, much of the water mass flows southward in a diffuse interior circulation south of the Denmark Strait[8], where it encounters the dramatic topography of the Mid-Atlantic Ridge. There, a complex network of fracture zones emanates from the rift valley where the North American and Eurasian/African tectonic plates diverge. Within the network of fracture zones and rift-valley segments, flows passing through constrictions and across sills accelerate to speeds much greater than the tidal or overlying geostrophic flows. The resulting overflows are often hydraulically controlled, with rapid conversion of potential to kinetic energy downstream of the controlling topography, and extremely large levels of turbulent mixing. While most past work has focused on overflows of prominent straits separating major basins (Denmark Strait[8]; Strait of Gibraltar[9]) and major deep fracture zones (Vema Passage[10], Romanche[6]), more recent work has indicated significant overflow processes acting in the smaller passages along the Mid-Atlantic Ridge[11–14]. Aside from the Romanche passage[6], and several turbulence profiles unintentionally collected downstream of sills in a deep fracture zone canyon[14], no direct measurements of mixing are available.

Motivated by the lack of direct measurements, we conducted a survey in the rift valley of the 'Lucky Strike' segment on the Mid-Atlantic Ridge (LS in Fig. 1). The geology of the site is being studied in the context of the French MoMAR (Monitoring the Mid-Atlantic Ridge) programme[15]. The GRAVILUCK cruise, carried out in August 2006 primarily to investigate details of the gravity field at Lucky Strike, provided a cruise opportunity for physical oceanographic measurements at a novel site. The survey focused on the narrow passage to the east of the Lucky Strike volcano (Fig. 1). The axial depth of the 7 km long eastern passage ranges from 2,200 m to 2,050 m at a sill. Below 1,800 m the passage is laterally constricted by the rift-valley wall in the east and by the eastern flank of the Lucky Strike volcano in the west; at 1,800 m its width at the latitude of the sill is roughly 3 km, and the mean steepness of the sidewalls is 0.3 (rise over run). We are unaware of any previous deep-ocean turbulence survey accomplished in such a narrow and steep passage.

The field survey used two instrument systems to characterize the hydrography, flow and turbulence. A deep microstructure profiler system (DMP), and a lowered acoustic Doppler current profiler system (ADCP) were used. Both incorporate conventional conductivity, temperature and depth (CTD) systems for hydrographic measurements. All DMP and lowered ADCP deployments were carried out simultaneously, allowing for concurrent measurements of turbulence and velocity in the passage. In addition to the lowered systems, a bottom-mounted ADCP was deployed by the submersible *Nautile* in close proximity to the sill. This additional unit recorded velocity for two weeks in the 100-m depth interval above the sill, giving an unambiguous record of the time-varying flow.

A combined hydrography and flow section showing cluster-averaged fields along the eastern passage is presented in Fig. 2. Profiles were made in clusters of two to five profiles each, at eight locations within the passage, corresponding to three upstream sites (U1 to U3), one at the sill, and four downstream (D1 to D4). The data show a mean northward flow, with strong shear below 1,800 m separating the flow through the passage from the circulation above. The velocity data indicate a marked acceleration at the sill, leading to mean downstream velocities exceeding $10\,cm\,s^{-1}$. The density structure across the passage has features typical of hydraulically controlled flows. Along the passage, isopycnals (neutral density contours; γ_n) slope significantly across the sill. Froude numbers, $Fr = V/(NH)$, were calculated along the passage from depth-averaged meridional velocities V, mean buoyancy frequencies N, and layer thicknesses H below 1,800 m.

[1]Department of Oceanography, Florida State University, Tallahassee, Florida 32306, USA. [2]Division of Ocean and Climate Physics, Lamont-Doherty Earth Observatory, Palisades, New York 10964, USA.

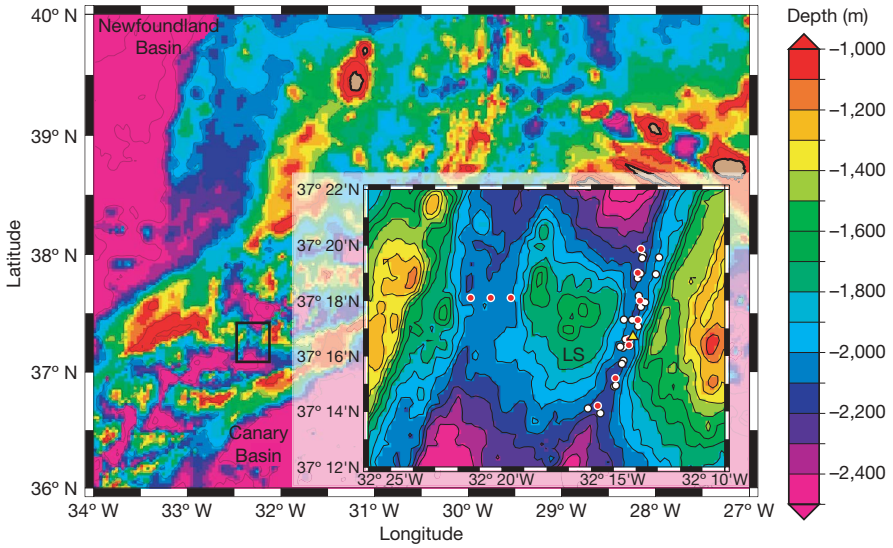

Figure 1 | Regional setting (box) and topography (inset) of the Lucky Strike segment. The main figure shows basin-scale bathymetric data[21], and the inset shows local survey bathymetric data[28]. The colour scheme is chosen to maximize contrast for the Mid-Atlantic Ridge axis. Measurement locations show lowered ADCP stations (white circles), DMP stations (red circles), and a bottom-mounted ADCP (yellow triangle).

Froude numbers reported in Fig. 2 show an abrupt increase to values near 1 at the sill and a similarly abrupt decrease between D2 and D3. This is suggestive of hydraulic control and, possibly, of a hydraulic jump downstream of the sill.

Density contours incrop along the passage floor, suggesting strong mixing, which was clearly indicated in the measurements of turbulent dissipation rate (Fig. 3). Dissipation rates reaching $\varepsilon \geq 10^{-8}\,\mathrm{W\,kg^{-1}}$ were observed throughout the depth interval of the passage, in contrast to typical thermocline levels of $\varepsilon = (1\text{–}3) \times 10^{-10}\,\mathrm{W\,kg^{-1}}$. Both upstream and downstream of the sill, dissipation levels are largest near the seabed, indicating the presence of an active bottom boundary layer. Upstream of the sill, elevated dissipation levels occur between 2,000 m and the sea bed, but they are generally below $10^{-8}\,\mathrm{W\,kg^{-1}}$. Just downstream of the sill, dissipation levels reach nearly $10^{-6}\,\mathrm{W\,kg^{-1}}$, as large as any observed in the abyssal ocean[6].

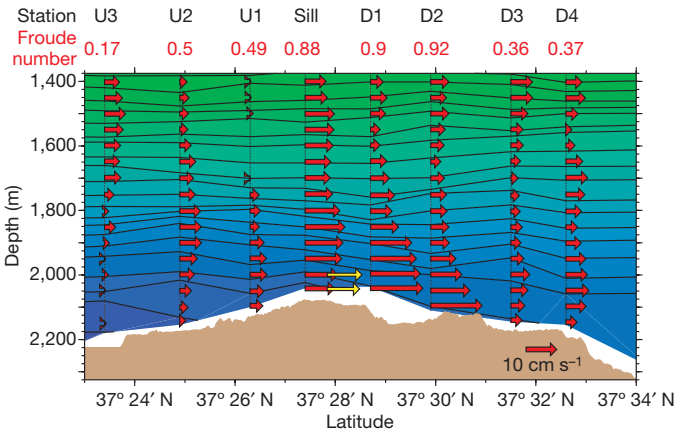

Figure 2 | Velocity and neutral-density contours along the deep passage east of the Lucky Strike volcano. Between U2 and D2, the passage is laterally closed below 1,800 m (Fig. 1). Average station locations upstream (U1 to U3), at the sill, and downstream (D1 to D4) are indicated along the upper edge of the figure; red numbers indicate the maximum Froude numbers below 1,800 m (see text for details). Red arrows, 50-m-averaged lowered ADCP data; yellow arrows, the two-week-averaged velocities recorded by a bottom-mounted ADCP. Irregularly spaced neutral density contours ranging from 27.852 to 27.952 $\mathrm{kg\,m^{-3}}$ were selected for approximately uniform spacing in depth.

Turbulent diffusivities were also calculated by averaging downstream, sill, and upstream DMP measurements. A model[16] assuming a constant mixing efficiency parameter of $\Gamma = 0.2$ was used to relate the diffusivity k_ρ to the dissipation rate and buoyancy gradient: $k_\rho = \Gamma\langle\varepsilon\rangle/\langle N^2\rangle$. Figure 4 shows these ensemble-averaged profiles. In all profiles diffusivities of $k_\rho \geq 1 \times 10^{-4}\,\mathrm{m^2\,s^{-1}}$ ($1\,\mathrm{cm^2\,s^{-1}}$) reach to levels 600 m above the passage bottom, that is, to the base of the main thermocline. Mixing is greatly enhanced within the passage, with diffusivities exceeding $k_\rho = 3 \times 10^{-3}\,\mathrm{m^2\,s^{-1}}$ ($30\,\mathrm{cm^2\,s^{-1}}$) within the bottom boundary layer. In particular, diffusivities just downstream of the sill reach $k_\rho \approx 3 \times 10^{-2}\,\mathrm{m^2\,s^{-1}}$ ($300\,\mathrm{cm^2\,s^{-1}}$) with a vertical density gradient of $N > 1 \times 10^{-3}\,\mathrm{s^{-1}}$, an order of magnitude greater than stratifications in abyssal fracture zones[6].

We are unaware of any previous observation of such large turbulence levels in significantly stratified deep water (below 1,000 m). A similar section of flow and turbulence was observed in the Romanche fracture zone[6], but that passage is the major connection between the North and South Atlantic basins, whereas the Lucky Strike passage connects two minor sub-basins in the rift valley of the Mid-Atlantic Ridge. Furthermore, the effects of overflow mixing in the Romanche fracture zone are limited to Antarctic Bottom Water, and thus do not directly affect the buoyancy of the main

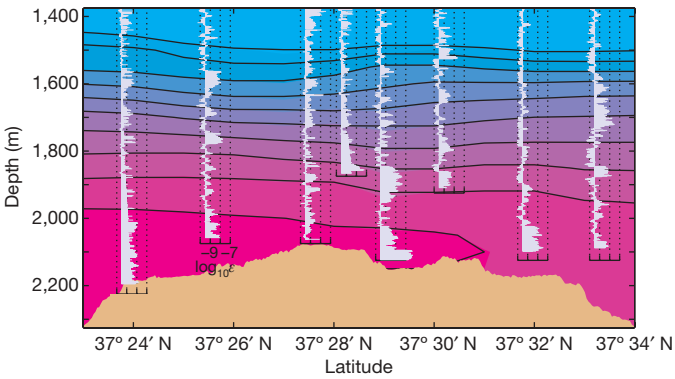

Figure 3 | Turbulence dissipation-rate profiles along the eastern passage at the Lucky Strike site. In all cases, a logarithmic axis is used, as indicated by the labelled example. Data are plotted about a reference level of $3 \times 10^{-10}\,\mathrm{W\,kg^{-1}}$, roughly corresponding to a background level of dissipation in the main thermocline. Contours show potential temperatures (relative to the sea surface) from 4.0 to 5.0 °C at 0.1 °C intervals.

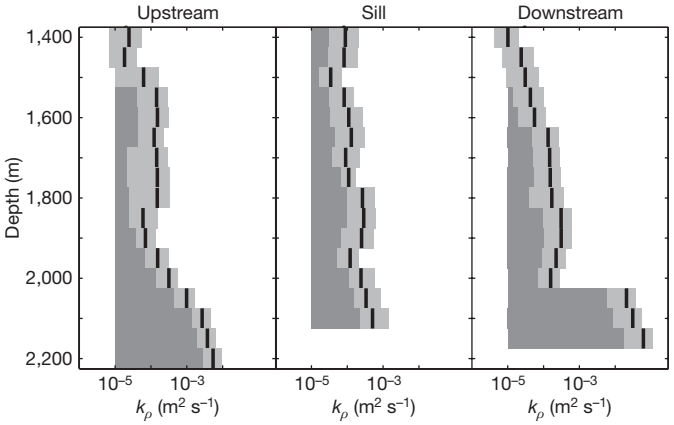

Figure 4 | Turbulent diffusivity estimates for station groups at the upstream, sill and downstream passage locations. Estimates were made in 50-m depth intervals, and mean values (dark line segments) and 95% confidence intervals (light-shaded band) are shown relative to a reference of $1 \times 10^{-5}\,m^2\,s^{-1}$, which is a typical thermocline mixing rate.

thermocline, which mostly involves North Atlantic Deep Water [17,18]. The processes acting at Lucky Strike are in contrast to those acting in abyssal fracture zones because, first, the site is shallow enough to allow enhanced mixing to extend into the well-stratified waters at the base of the thermocline, and second, although it is small in spatial extent, the Lucky Strike passage is typical of many thousands of similar sites through the global mid-ocean ridge canyon network[14].

Water mass conversion at Lucky Strike can be assessed by estimating the buoyancy flux occurring in the passage, $F = Q\Delta\rho \approx 2 \times 10^3\,kg\,s^{-1}$, where Q is the along-valley volume flux and $\Delta\rho$ is the deep cross-sill density difference[7]. Persistent northward flow in the continuous rift valley between 35.5° N and 37.5° N has been observed at several latitudes[12,13,19] and the monotonically decreasing rift-valley density in the same region[20] suggests that this northward flow is continuous. Topographic data indicate that, within this 250 km of rift valley, the water must flow through at least nine passages. Unambiguous evidence for overflows is available from four of those locations[12,13,19], and overflows probably occur in all. Taken together, the buoyancy flux associated with overflows in this short 2° stretch of the Mid-Atlantic Ridge rift valley equals a tenth of that occurring at the Romanche fracture zone[7]. Scaled over the greater North Atlantic Mid-Atlantic Ridge, this result suggests that overflows in the rift valley alone account for as much water mass conversion as is occurring at Romanche.

The large-scale effects of water mass conversion at Lucky Strike can also be assessed by examining the influence of rift-valley and ridge-flank mixing on the North Atlantic basin as a whole. From an analysis of bathymetric data[21] for the region between 20° N and 60° N, we find that just over 3% of the basin area bounded by the 2,000-m isobath on the continental slopes contains ridge topography shallower than 2,000 m. Treating this ridge topography as similar to the Lucky Strike region, we assume that diffusivities of $k_\rho = 3 \times 10^{-4}\,m^2\,s^{-1}$ ($3\,cm^2\,s^{-1}$) characterize the mixing in and above the narrow passages constricting the flow. If the regions away from mid-ocean ridge locations are assumed to have a diffusivity of $k_\rho \approx 1 \times 10^{-5}\,m^2\,s^{-1}$ ($0.1\,cm^2\,s^{-1}$) (ref. 5), then the 3% of the deep basin area occupied by ridges and their associated passages contributes the same area-integrated diapycnal buoyancy flux as the rest of the basin.

METHODS

Lowered acoustic Doppler profile data for velocity, and CTD hydrographic data were analysed using methods now common in the oceanographic community[22,23]. The DMP is a specialized free-falling, autonomous, vertical microstructure system made by Rockland Scientific International. Specifications for the system can be found online[24]. Of specific interest is the measurement of microstructure shear used in the quantification of turbulent kinetic energy ε. This is the rate of energy removal by the molecular viscosity of sea water ν acting on the mean-square turbulent shear $\langle u_z^2 \rangle$, and is used in the relation $\varepsilon = (15/2)\nu\langle u_z^2 \rangle$ (ref. 25). Analysis of the shear signal is done using spectral analysis[26] over 1-m depth intervals of the microstructure record. For each ε estimate, shear variance $\langle u_z^2 \rangle$ is computed using a spectral integration. Estimates of diffusivity were made for 50-m profile segments, as reported in Fig. 4. Confidence intervals were computed using a bootstrap method applied to each 50-m segment[27].

Lowered ADCP and CTD data. A Teledyne RD Instruments 300 kHz Workhorse ADCP was used in conjunction with a Seabird 911 CTD on a 24-bottle rosette frame. Bottle samples were used to verify the accuracy of this CTD's salinity calibration, which is better than 0.002. In addition to the lowered ADCP profiles done in conjunction with the DMP, 18 additional full-depth profiles were collected in the eastern passage (Fig. 1). Resampling of the eastern passage was done roughly every four days, with the full observational record extending over three weeks. These were timed to sample the semidiurnal tidal cycle as completely as possible. The excellent correspondence between the time-averaged velocities recorded by the bottom-mounted ADCP (also a Teledyne RD Instruments 300 kHz Workhorse) near the sill (yellow arrows) and the nearby cluster-averaged lowered ADCP profile suggests that Fig. 2 closely approximates a temporal average. Thus, the available hydrographic and velocity measurements capture the tidal variability associated with the spring–neap cycle.

Dissipation data. The DMP instrument system was designed to match the general specifications of the several other full-depth capable microstructure systems in use by the ocean turbulence community. In addition to a Seabird CTD system, the DMP uses up to six microstructure sensors to determine the turbulent mixing rates. The profiler samples turbulent shear at 512 Hz as it descends at roughly $0.6\,m\,s^{-1}$, achieving a vertical full-wavelength resolution of 3 mm. The raw shear signal is processed using well-documented techniques[25]. Electronic noise, instrument vibration, and small amounts of turbulence generated at the leading edge of the guard assembly apply a shear dissipation rate noise level of $1 \times 10^{-10}\,W\,kg^{-1}$ to our measurements. Ensemble averages over non-overlapping 50-m profile segments are used in the estimates for diffusivities. Dissipation statistics in each 50-m segment are treated as containing five degrees of freedom, based on taking 10 m as the average turbulence patch scale. It follows that each Monte Carlo bootstrap sampling of the 50-m segment data contains five ε values, drawn with replacement[27].

Received 9 February; accepted 21 June 2007.

1. Munk, W. H. Abyssal recipes. *Deep-Sea Res.* **13,** 207–230 (1966).
2. Munk, W. & Wunsch, C. Abyssal recipes. II: Energetics of tidal and wind mixing. *Deep-Sea Res.* **45,** 1977–2010 (1998).
3. Munk, W. in *Evolution of Physical Oceanography* 264–291 (The MIT Press, Cambridge, 1981).
4. St Laurent, L. C. & Garrett, C. The role of internal tides in mixing the deep ocean. *J. Phys. Oceanogr.* **32,** 2882–2899 (2002).
5. Kunze, E. & Sanford, T. B. Abyssal mixing: where it is not. *J. Phys. Oceanogr.* **26,** 2286–2296 (1996).
6. Polzin, K. L., Speer, K. G., Toole, J. M. & Schmitt, R. W. Intense mixing of Antarctic Bottom Water in the equatorial Atlantic Ocean. *Nature* **380,** 54–57 (1996).
7. Bryden, H. L. & Nurser, A. J. G. Effects of strait mixing on ocean stratification. *J. Phys. Oceanogr.* **33,** 1870–1872 (2003).
8. Girton, J. B. & Sanford, T. B. Descent and modification of the overflow plume in the Denmark Strait. *J. Phys. Oceanogr.* **33,** 1351–1364 (2003).
9. Farmer, D. & Armi, L. The flow of Mediterranean water through the Strait of Gibraltar. *Prog. Oceanogr.* **21,** 1–105 (1988).
10. Hogg, N. G., Biscaye, P., Gardner, E. & Schmitz, W. J. On the transport of Antarctic Bottom Water in the Vema Channel. *J. Mar. Res.* **40** (Suppl.), 231–263 (1982).
11. Thurnherr, A. M. Diapycnal mixing associated with an overflow in a deep submarine canyon. *Deep-Sea Res. II* **53,** 194–206 (2006).
12. Thurnherr, A. M. & Richards, K. R. Hydrography and high-temperature heat flux of the rainbow hydrothermal site (36:14N, Mid-Atlantic Ridge). *J. Geophys. Res.* **106,** 9411–9426 (2001).
13. Thurnherr, A. M., Richards, K. J., German, C. R., Lane-Serff, G. F. & Speer, K. G. Flow and mixing in the rift valley of the Mid-Atlantic Ridge. *J. Phys. Oceanogr.* **32,** 1763–1778 (2002).
14. Thurnherr, A. M., St Laurent, L. C., Speer, K. G., Toole, J. M. & Ledwell, J. R. Mixing associated with sills in a canyon on the mid-ocean ridge flank. *J. Phys. Oceanogr.* **35,** 1370–1381 (2005).
15. Escartin, J. *Monitoring the Mid-Atlantic Ridge (MoMAR)* ⟨http://www.ipgp.jussieu.fr/rech/lgm/MOMAR/⟩ (2006).
16. Osborn, T. R. Estimates of the local rate of vertical diffusion from dissipation measurements. *J. Phys. Oceanogr.* **10,** 83–89 (1980).
17. Webb, D. J. & Suginohara, N. Vertical mixing in the ocean. *Nature* **409,** 37 (2001).

18. St Laurent, L. & Simmons, H. L. Estimates of power consumed by mixing in the ocean interior. *J. Clim.* **19,** 4877–4890 (2006).
19. Keller, G. H., Anderson, S. H. & Lavelle, J. W. Near-bottom currents in the Mid-Atlantic Ridge rift valley. *Can. J. Earth Sci.* **12,** 703–710 (1975).
20. Wilson, C., Speer, K., Charlou, J.-L., Bougault, H. & Klinkhammer, G. Hydrography above the Mid-Atlantic Ridge (33°-40°N) and within the Lucky Strike segment. *J. Geophys. Res.* **100,** 20555–20564 (1995).
21. Smith, D. K. & Sandwell, D. Global sea floor topography from satellite altimetry and ship depth soundings. *Science* **277,** 1956–1962 (1997).
22. Joyce, C. & Corry, C. *WHP 90–1: Requirements for WOCE Hydrographic Program Data Reporting* ⟨http://cchdo.ucsd.edu/manuals.htm⟩ (1994).
23. Visbeck, M. Deep velocity profiling using lowered acoustic Doppler current profiler: bottom track and inverse solutions. *J. Atmos. Ocean. Technol.* **19,** 794–807 (2002).
24. Rockland Scientific International. *Microstructure Instruments—VMP 5500* ⟨http://www.rocklandscientific.com/products_vmp5500.php⟩ (2006).
25. Lueck, R. G., Wolk, F. & Yamazaki, H. Oceanic velocity microstructure measurements in the 20th century. *J. Oceanogr.* **58,** 153–174 (2002).
26. Gregg, M. C. Uncertainties and limitations in measuring ε and χ. *J. Atmos. Ocean. Technol.* **16,** 1483–1490 (1999).
27. Emery, W. J. & Thomson, R. E. *Data Analysis Methods in Physical Oceanography* (Elsevier Science, Amsterdam, 2001).
28. Cannat, M. *et al.* Mid-Atlantic Ridge-Azores hotspot interactions: Along-axis migration of a hotspot-derived event of enhanced magmatism 10 to 4 Ma ago. *Earth Planet. Sci. Lett.* **173,** 257–269 (1999).

Acknowledgements We thank V. Ballu for inviting us to join the GRAVILUCK cruise. We also thank P. Bouruet-Aubertot, G. Reverdin, and the scientific staff and crew of the N/O *Atalante* for their assistance during the field programme. Technical support of the DMP by R. Lueck, F. Wolk, and P. Stern of Rockland Scientific, and by E. Howarth of FSU, was invaluable. E. Kunze provided comments on the early draft of the manuscript. The FSU turbulence instrumentation programme is supported by the US Office of Naval Research. The LDEO lowered ADCP programme, and our participation in GRAVILUCK, was sponsored by the US National Science Foundation.

Author Contributions L.C.StL. and A.M.T. contributed equally to this work. L.C.StL. led the microstructure sampling programme, and analysed the turbulence data. A.M.T. led the lowered ADCP measurement programme, and analysed the velocity data.

Author Information Reprints and permissions information is available at www.nature.com/reprints. The authors declare no competing financial interests. Correspondence and requests for materials should be addressed to to L.C.StL. (stlaurent@ocean.fsu.edu).